Lewis Superacidic Heavy Pnictaalkene Cations: Comparative Assessment of Carbodicarbene-Stibenium and -Bismuthenium Ions

Levi S. Warring,[a] *Jacob E. Walley,*[a] *Diane A. Dickie,*[a] *William Tiznado,*[b] *Sudip Pan,*[*c,d] *and Robert J. Gilliard, Jr.* [*a]

[a] Department of Chemistry, University of Virginia, McCormick Road, PO Box 400319, Charlottesville, Virginia 22904, USA. E-mail: rjg8s@virginia.edu

[b] Computational and Theoretical Chemistry Group, Departamento de Ciencias Químicas, Facultad de Ciencias Exactas, Universidad Andres Bello, República 270, Santiago, 8370146, Chile.

[c] Philipps-Universität Marburg Hans-Meerwein-Straße, Marburg, 35032, Germany. E-mail: pans@chemie.uni-marburg.de

[d]Institute of Atomic and Molecular Physics, Jilin University, Changchun 130023, China

ABSTRACT

We report a comprehensive assessment of the Lewis acidity for a series of carbone-stibenium and -bismuthenium ions using the Gutmann-Beckett method. These new antimony and bismuth cations have been synthesized by halide abstractions from (CDC)$PnBr_3$ and [(^{py}CDC)$PnBr_2$][Br] (CDC = carbodicarbene; Pn = Sb or Bi; py = pyridyl). The reaction of (CDC)$SbBr_3$ (**1**) with one or two equivalents of $AgNTf_2$ (NTf_2 = bis(trifluoromethanesulfonyl)imide) or $AgSbF_6$ gives stibaalkene mono- and di-cations of the form [(CDC)$SbBr_{3-n}$][A]$_n$ (**2-4**; n = 1,2; A = NTf_2 or SbF_6). The stibaalkene trication [$(CDC)_2Sb$][NTf_2]$_3$ (**5**) was also isolated and collectively these molecules fill the gap among the series of cationic pnictaalkenes. The Sb cations are compared to the related CDC-bismaalkene complexes **6**-**9**. With the goal of preparing highly Lewis acidic compounds, a tridentate bis(pyridine)carbodicarbene (^{py}CDC) was used as a ligand to access [(^{py}CDC)$PnBr_2$][Br] (**10**, **12**) and trications [(^{py}CDC)Pn][NTf_2]$_3$ (Pn = Sb (**11**), Bi (**13**)), forgoing the need for a second CDC as used in the synthesis of **5**. The bonding situation in these complexes is elucidated through electron density and energy decomposition analyses in combination with natural orbital for chemical valence theory. In each complex there exists a CDC-Pn double bonding interaction, consisting of a strong σ-bond and a weaker π-bond, whereby the π-bond gradually strengthens with the increase in cationic charge in the complex. Notably, [(CDC)SbBr][NTf_2]$_2$ (**4**) has an acceptor number (84) that is comparable to quintessential Lewis acids such as BF_3, and

tricationic pnictaalkene complexes **11** and **13** exhibit strong Lewis acidity with acceptor numbers of 109 (Pn = Sb) and 84 (Pn = Bi), respectively, which are among the highest values reported for any antimony or bismuth cation. Moreover, calculated fluoride ion affinities for **11** and **13** are 99.8 and 94.3 kcal/mol, respectively, which are larger than SbF_5 (85.1 kcal/mol), which suggest these cations Lewis superacids.

INTRODUCTION

There has been an increased interest in the chemistry of compounds containing the heavy pnictogen elements (Sb and Bi) due to the development of redox active or Lewis acidic molecules that mediate key organic transformations.[1-6] However, Sb and Bi exhibit stark differences in bonding compared to the lighter group 15 elements (P, As), and thus, structurally analogous compounds tend to be substantially more reactive. These differences in reactivity can be attributed to several factors: the increase in covalent and van der Waals radii moving from N to Bi,[7, 8] a change in the radial extension between the *s* and *p* orbitals moving down the group,[9] and the increase in the one-electron ionization energies.[10] A common synthetic strategy that has been employed to tame the reactivity of organometallic Sb and Bi complexes typically involves using sterically demanding anionic ligand systems that form strong carbon- and/or nitrogen-pnictogen bonds (e.g., N,C,N-pincer). Using these systems, Cornella demonstrated the redox cycling capability of bismuth for transformations of organic substrates and small molecules (e.g., nitrous oxide), opening the door to new possibilities in main-group element-mediated catalysis.[11-14]

We have been interested in understanding matters of chemical bonding and stability in systems where Sb or Bi is stabilized by neutral donor ligands. While there are a plethora of compounds containing L-type carbon-based ligands bound to P and As, analogous Sb and Bi compounds are exceptionally rare.[15-22] We reduced carbene-Bi(III) halides and isolated the first carbene-bismuthinidene, but those compounds were isolated in relatively low yields and were significantly more reactive than their lighter congeners.[23, 24] As an alternative strategy, we then pursued highly electrophilic cations as a new platform for reaction chemistry. Antimony cations have already been shown to perform transfer hydrogenation in organic molecules.[25, 26] In addition, the conversion of aldehydes into symmetric ethers, α, β-unsaturated aldehydes and 1,3,5-trioxanes has been realized with a cationic antimony(V) catalyst.[27] The propensity of these cations to activate chemical bonds is often dictated by their Lewis acidity,[28-30] but to the best of our knowledge, there have been no reports of bond activation in compounds that feature C→Sb^+ or C→Bi^+ centers. This may be attributed to the fact that it has remained unclear how to access well-defined compounds that are both highly Lewis acidic and thermally stable.

The utilization of carbones[31, 32] as a ligand in main-group chemistry is an emerging strategy to access molecules with carbon-heteroatom multiple bonding.[31, 33-43] Kuzu and coworkers reported the first examples of carbodiphosphorane (CDP) adducts of $SbCl_3$ and $BiCl_3$ (Figure 1, **A**), with short ^{carbone}C–Pn (Pn = Sb or Bi) bonds, as well as a CDP-stabilized Bi dication (Figure 1, **B**).[33] Wesemann and coworkers utilized a dianionic *N,C,N* pincer-type

ligand to attain a C=Bi double bond (Figure 1, **C**).[44] Recently, we reported a series of carbodicarbene (CDC)-stabilized bismaalkene cations (Figure 1, **D**).[35] It is noteworthy that carbones impart thermal stability in these low-coordinate donor-stabilized heavy pnictogen compounds that could not be achieved with standard carbenes.[24, 35] Herein, we report the synthesis, molecular structures, computations, and Lewis acidity assessment of mono-, di-, and tri-cationic CDC-stibenium and bismuthenium ions (Figure 1, **E**). Not only is this the first quantitative assessment of Lewis acidity for heavy element carbone-pnictenium ions, but C=Sb^{+}, C=Sb^{2+}, and C=Sb^{3+} compounds with strong multiple bond character are hitherto unknown, with antimony representing the only missing element from the cationic pnictaalkene family. Considering the reports from Pellois and Gabbaï[45] and Venugopal[46] who observed a reversal in the Lewis acidity trend for Sb and Bi, we were particularly interested in accessing these molecules. Notably, the Gutmann-Beckett acceptor numbers (AN) for the pyridyl-substituted CDC-Sb^{3+} and CDC-Bi^{3+} complexes are among the highest observed for any cationic antimony or bismuth compound in the literature, and based on fluoride ion affinities they may be considered Lewis superacids.

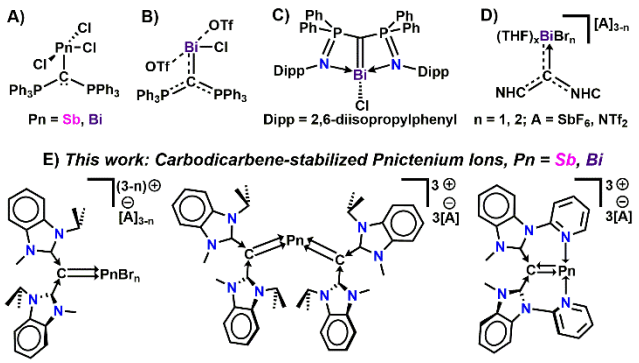

Figure 1. A) Carbodiphosphorane (CDP)-coordinated $PnCl_3$ complexes, **B**) a CDP-stabilized bismuth dication **C**) Dianionic *N,C,N*-pincer ligand supporting a C=Bi double bond, and **D**) Carbodicarbene (CDC)-bismaalkene cations, **E**) CDC-pnictaalkene cation (Pn = Sb, Bi) Lewis acidity (this work).

RESULTS AND DISCUSSION

Carbodicarbene (CDC)[47] was reacted with $SbBr_3$ in THF at room temperature to afford (CDC)$SbBr_3$ (**1**) as a yellow solid in >99% yield after workup. A well-defined heptet at 4.96 ppm in the ^1H NMR spectrum of **1** in CD_2Cl_2 corresponds to the methine proton of CDC in a new coordination environment. Yellow crystals suitable for X-ray diffraction studies were obtained from layered diffusion of diethyl ether into a solution of **1** in dichloromethane (DCM) (Figure 2). The molecular structure of **1** reveals a four-coordinate complex where the Sb atom is in a distorted see-saw geometry. One or two equivalents of the halide abstraction reagent $AgSbF_6$ or $AgNTf_2$ (NTf_2 = bis(trifluoromethylsulfonyl)imide) were added to a solution of **1** in DCM to give mono- and dicationic CDC–Sb complexes [(CDC)$SbBr_2$][SbF_6] (**2**), [(CDC)SbBr][SbF_6]$_2$ (**3**), and [(CDC)SbBr][NTf_2]$_2$ (**4**) (Scheme 1). While there are numerous ways to represent these molecules, for the schemes we have chosen both simplified zwitterionic and dative bonding conventions. A more detailed discussion of the bonding is provided in the computational section. New, upfield ^1H NMR resonances in CD_2Cl_2 were observed for the methine protons in compounds **2** (4.79 ppm) and **4** (4.81 ppm) compared to **1** (4.96 ppm), indicating the formation of new coordination compounds.[48] Adding a third equivalent of $AgNTf_2$ to **1** did not lead to a third bromide abstraction;

therefore, we posited that an additional ligand was necessary to prepare an antimony trication. Indeed, the addition of one equivalent of CDC to (CDC)$SbBr_3$, followed by the addition of three equivalents of $AgNTf_2$ afforded tricationic $[(CDC)_2Sb][NTf_2]_3$ (**5**) (Scheme 1). Spectroscopic analysis by ^1H NMR showed two CDC ligand environments as evidenced by the formation of two new methine resonances in the ^1H NMR spectrum at 5.92 and 4.56 ppm in CD_2Cl_2. This suggests that one of the methine protons is oriented in a favorable position to interact weakly with antimony, which would deshield the methine proton and contribute to the observed downfield ^1H NMR chemical shift. Additionally, two *N*-methyl signals are observed for the trication, indicating inequivalent ligand environments. The distinct methine and *N*-methyl resonances on CDC indicate that rotation of the ligands along the $^{carbone}C$–Sb bond is sterically hindered. Contrarily, the observation of single methine resonances in the mono- and di-cations suggests that there is free rotation along the $^{carbone}C$–Sb bond. ^{13}C NMR spectroscopy shows downfield shifts for the ^{NHC}C atoms in the cations compared to uncoordinated CDC (152.3-156.9 ppm for **1**, **2**, **4** and **5** in CD_2Cl_2 vs. 142.3 ppm for free CDC in C_6D_6). These downfield shifts are indicative of strong donation from the carbone carbon to antimony.

Scheme 1. Synthetic routes to isolate cationic carbodicarbene-antimony complexes. The bonding situations in these cations is depicted using conventional zwitterionic and dative bonding representations (**2**-**4**), as both are common in the literature. However, any one structure should be considered limiting and a detailed bonding analysis using energy

decomposition analysis in combination with natural orbitals for chemical valence (EDA-NOCV) is provided *vide infra*.

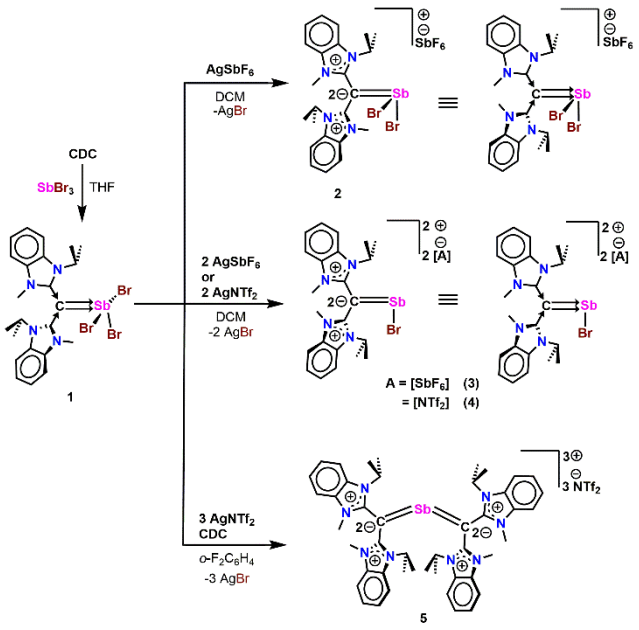

The solid-state structures of compounds **1**-**5** are shown in Figure 2. Yellow crystals of **1** were isolated from a layered mixture of hexanes/DCM. Compound **1** has a short ^{carbone}C–Sb bond (2.089(13) Å), which is comparable to the ^{carbone}C–Sb bond (2.15(1) Å) reported in the (CDP)$SbCl_3$ complex by Kuzu and coworkers.[33] Yellow and red crystals suitable for X-ray diffraction studies were grown from layered diffusion of hexanes into concentrated solutions of **2**, **3**, and **4** in DCM, respectively. Due to the poor quality of crystals for compound **3**, bond parameters are not discussed in detail. However, the atom determination and connectectivity in the structure are unambiguous. Short ^{carbone}C–Sb bonds are observed for cations **2**-**5** (2.039-2.090 Å) and compound **4** has the shortest C–Sb bond (2.0392(16) Å) reported for a Sb cation. In each cation, the ^{carbone}C–Sb bond is shorter than the sum of covalent radii for a C–Sb single

bond (2.15 Å).[7] Additionally, the average $^{NHC}C–^{carbone}C$ bond in the monocation (1.436 Å), dication **4** (1.457 Å), and trication (1.448 Å and 1.450 Å) is significantly longer compared to the uncoordinated CDC (1.335(5) Å),[47] indicating a decrease in the double bond character of the $^{NHC}C–^{carbone}C$ moiety. The short C–Sb bonds and lengthened $^{NHC}C–^{carbone}C$ bonds support the classification of these cations as stibaalkenes.

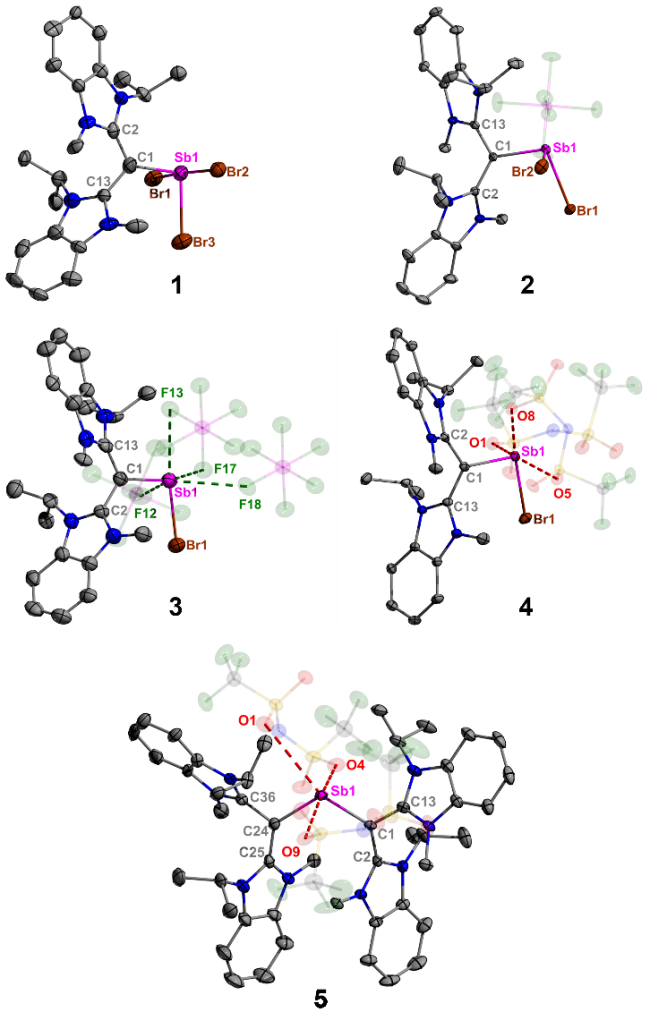

Figure 2. Molecular structures of compounds **1**-**5**. Thermal ellipsoids are set at the 50% probability for **1**, **2**, **4**, and **5**, 30% for **3**. H atoms and solvent molecules are omitted for clarity. A non-coordinating triflimide anion is omitted for clarity in **5**. Selected bond lengths (Å) and

angles (°) for **1**: Sb1–C1: 2.089(13) Sb1–Br1: 2.7729(15); Sb1–Br2: 2.8603(16); Sb1–Br3: 2.5207(16); C1–C2: 1.438(18); C1–C13: 1.476(17); C2–C1–C13: 112.3(11); C1–Sb1–Br1: 94.1(4); C1–Sb1–Br2: 93.6(4); C1–Sb1–Br3: 98.5(4); Br1–Sb1–Br2: 172.33(5); Br1–Sb1–Br3: 86.67(5), **2**: Sb1–C1: 2.090(2); Sb1–Br1: 2.5080(5); Sb1–Br2: 2.5872(5); 2.860; C1–C2: 1.453(3); C1–C13: 1.418(3); C2–C1–C13: 121.1(2); C1–Sb1–Br1: 98.58(7); C1–Sb1–Br2: 99.95(7); Br1–Sb1–Br2: 91.396(14), **3**: Sb1–C1: 2.06(2); Sb1–Br1: 2.469(3); C1–C2: 1.49(3); C1–C13: 1.40(3); C2–C1–C13: 121(2); C1–Sb1–Br1: 98.1(7), **4**: Sb1–C1: 2.0392(16); Sb1–Br1: 2.4990(2); C1–C2: 1.454(2); C1–C13: 1.459(2); C2–C1–C13: 121.36(14); C1–Sb1–Br1: 95.59(5), **5**: Sb1–C1: 2.059(2); Sb1–C24: 2.064(2); C1–C2: 1.442(3); C1–C13: 1.453(3); C2–C1–C13: 114.99(17); C2–C1–Sb1: 131.08(14).

The solid-state structures of compounds **2**-**5** show weak anion coordination to antimony, which is unsurprising given that they are electrophilic, and the stabilization of reactive p-block compounds by weakly coordinating anions is well-documented.[49] The $[SbF_6]^-$ anion contact to Sb in **2** is 3.3423(19) Å, which is shorter than the sum of van der Waals radii for Sb and F (3.52 Å) but longer than the sum of covalent radii (2.04 Å).[7, 8] The dication **4** has significant contacts between Sb and the triflimide anions. Specifically, there are three Sb---O contacts, the shortest distance being 2.5658(13) Å, which is much longer than the sum of covalent radii (2.03 Å).[7] The two other contacts are slightly longer at 2.6595(14) and 3.0002(14) Å. The nearest $[NTf_2]^-$ contact to Sb in **5** is a sulfonyl oxygen atom that is 3.013(7) Å away. The electronic stabilization between the triflimide anions and

antimony is likely weak in **5** due to steric hindrance and electronic stabilization provided by the two strongly donating CDC ligands.

Analogous CDC-bismuthenium ions were also prepared. The mono-, di-, and tri-cations are nearly identical to those we reported previously;[35] however, we have modified the syntheses to prevent THF coordination to the bismuth centers in **7** and **8**.

In the interest of preparing highly Lewis acidic tricationic complexes, we selected the bis(pyridine)carbodicarbene (^{py}CDC) ligand first reported by Ong and coworkers, which is capable of acting as a tridentate ligand.[50] We rationalized that the pyridyl nitrogen atoms would coordinate to the electrophilic pnictogen centers, and provide sufficient electronic stabilization to promote a third halide abstraction without requiring a second equivalent of CDC ligand. As the pyridyl substituents are significantly weaker donors compared to CDC, our hypothesis was that this strategy would lead to complexes with enhanced Lewis acidity. Addition of ^{py}CDC to $SbBr_3$ in THF led to the formation of a yellow precipitate. Removal of solvent *in vacuo* gave [(^{py}CDC)$SbBr_2$][Br] (**10**) as a yellow solid in >99% yield. Compound **11,** [(^{py}CDC)Sb][NTf_2]$_3$, was prepared by the addition of three equivalents of $AgNTf_2$ to a solution of **10** in 1,2-difluorobenzene (Scheme 2).

Scheme 2. Synthetic route to prepare mono- and tricationic, ^{py}CDC-stabilized heavy pnictaalkene cations. Compounds **10** and **12** can similarly be represented by their zwitterionic structures similar to those drawn in Scheme 1. Compounds **11** and **13** are best represented by a sigma dative bond from CDC to Pn with a dative pi-backbond from Pn to CDC.

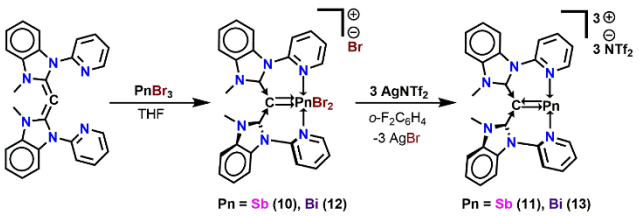

NMR data was collected in CD_3CN for **10** and **11** as both complexes are poorly soluble in CD_2Cl_2. The resonances for the protons *ortho* to the pyridyl nitrogen atoms are similar between **10** (9.01 ppm) and **11** (8.97 ppm). In contrast, the *N*-methyl protons are shifted downfield (3.37 ppm) in **11** compared to **10** (3.25 ppm). The bismuth analog of **10** was prepared by adding ^{py}CDC to $BiBr_3$ in THF to afford [(^{py}CDC)$BiBr_2$][Br] (**12**) as a red-orange solid in quantitative yield (Scheme 2). Compound **12** is insoluble in both CD_2Cl_2 and CD_3CN; however, it is partially soluble in CD_3OD. A doublet at 9.17 ppm in the ^{1}H NMR spectrum of **12** in CD_3OD corresponds to the protons *ortho* to the pyridyl nitrogen atoms on ^{py}CDC. Compound **13**, [(^{py}CDC)Bi][NTf_2]$_3$, was prepared by reacting **12** with three equivalents of $AgNTf_2$ in 1,2-difluorobenzene to give the product as a red solid (Scheme 2).

The solid-state structures of **10**-**13** are shown in Figure 3. Single crystals of **10** were isolated from a layered mixture of diethyl ether and DCM. Interestingly, **10** exists as a monocation with a bromide anion and tridentate coordination of ^{py}CDC to Sb. The ^{carbone}C–Sb bond is 2.134(11) Å, which is longer than those of compounds **1**-**5**. The lengthened ^{carbone}C–Sb bond can be attributed to the coordination of both pyridyl nitrogen atoms to Sb (average Sb–N distance of 2.369 Å). Orange crystals suitable for X-ray diffraction studies for **11** were obtained from layered diffusion of hexanes into a concentrated solution of 1,2-difluorobenzene. A shortening of the ^{carbone}C–Sb bond (2.071(8) Å) relative to **10** (2.134(11) Å)

is observed, but their Sb–N distances are identical within standard deviation. Similar to the stibaalkene cations **2**-**5**, there are triflimide anion contacts to Sb. Specifically, there are two equal Sb---O contacts with a distance of 2.330(14) Å, which is indicative of significant electronic stabilization from the triflimides to Sb.

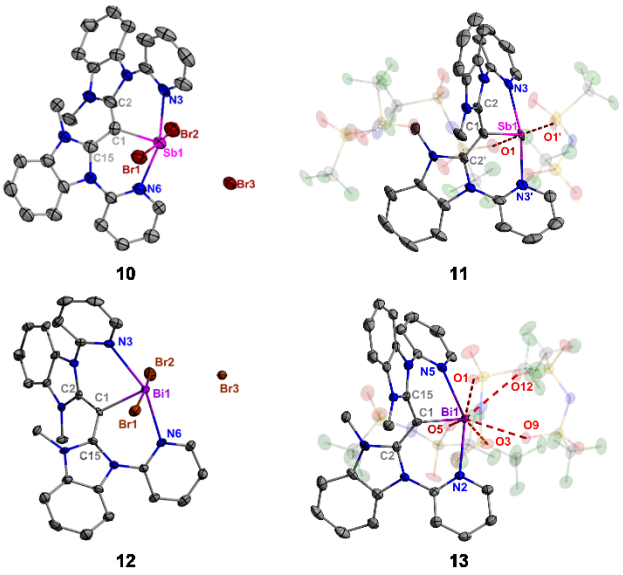

Figure 3. Molecular structures of compounds **10**-**13**. Thermal ellipsoids set at 50% probability level. H atoms omitted for clarity. Two DCM solvent molecules omitted for clarity for **10** and **12**, and a disordered 1,2-difluorobenzene molecule is omitted for **13**. Selected bond lengths (Å) and angles (°) for **10**: C1–Sb1: 2.134(11); Sb1–Br1: 2.7923(14); Sb1–Br2: 2.7077(14); C1–C2: 1.385(15); C1–C15: 1.390(14); N3–Sb1: 2.406(8); N6–Sb1: 2.332(7); C2–C1–C15: 121.5(10); N3–Sb1–C1: 80.3(3); C1–Sb1–Br1: 86.2(3), **11**: C1–Sb1: 2.071(8); C1–C2: 1.409(7); N3–Sb1: 2.355(6); C2–C1–C2': 120.430; N3–Sb1–C1: 82.36(12), **12**: C1–Bi1: 2.251(6); Bi1–Br1: 2.8543(7); Bi1–Br2: 2.7853(7); C1–C2: 1.388(9); C1–C15: 1.392(9); N3–Bi1: 2.506(5); N6–Bi1: 2.432(5); C2–C1–C15: 123.5(5); N3–Bi1–C1: 79.4(2); C1–Bi1–Br1: 86.82(16), **13**: C1–Bi1: 2.191(5); C1–

C2: 1.388(6); C1–C15: 1.410(6); N2–Bi1: 2.431(4); N5–Bi1: 2.495(4); C2–C1–C15: 120.9(4); N2–Bi1–C1: 81.98(15).

Orange crystals of **12** suitable for X-ray diffraction were grown from a layered mixture of hexanes/DCM. Compound **12** has a ^{carbone}C–Bi bond length of 2.251(6) Å, which is in line with previously reported carbone-bismuth complexes (2.157-2.280 Å).[33, 35] Like **10**, a bromide ligand has been displaced (3.3754(7) Å from Bi) due to pyridyl coordination to bismuth. Red crystals suitable for X-ray diffraction were grown from layer diffusion of hexanes into a concentrated solution of **13** in 1,2-difluorobenzene. The ^{carbone}C–Bi bond of 2.191(5) Å of **13** is shorter than that in **12** (2.251(6) Å). Unsurprisingly, there is significant triflimide anion coordination to Bi, with the shortest Bi---O contact being 2.409(3) Å.

Enhancing the Lewis acidity at the pnictogen center typically enhances the reactivity of pnictenium ions.[51] The Lewis acidity of p-block compounds has been evaluated using a variety of methods, including fluoride ion affinity,[52, 53] hydride ion affinity,[54] and the Gutmann-Beckett method.[55-57] The Gutmann-Beckett (GB) method is an experimental technique that measures the change in the ^{31}P NMR chemical shift of triethylphosphine oxide (O=PEt$_3$) after it is added to the sample of interest, which translates to an acceptor number (AN) using the following formula AN = 2.21 x [$\delta(^{31}\text{P NMR})_{sample}$ – 41.0].[58, 59] Comparative methods using softer bases (*e.g.,* S=PMe$_3$, Se=PMe$_3$) have also been used to evaluate the Lewis acidity of heavy group 15 complexes.[60, 61] Greb and Erdmann highlighted that the GB method is most reliable as a comparative tool for complexes that contain the same central elements and comparable ligands.[62]

Catalytically active antimony and bismuth complexes generally have reported acceptor numbers (ANs) greater than 50 as evaluated using the Gutmann-Beckett method.[63] For instance, the potent Lewis acid catalyst $BiCl_3$, which is used in many organic transformations, has an acceptor number of 49.[64-66] Recently, the Lewis acidity of several Sb and Bi cations has been evaluated using the Gutmann-Beckett method. Venugopal and coworkers observed a reversal in the Lewis acidity of bis(mesityl) antimony and bismuth compounds when the chloride substituent is replaced with triflate (Figure 4, **a**).[46] They also observed an increase in Lewis acidity as ligand bite angle decreased, whereby the acceptor number of **b** increased from 55 to 69 when the chelating ligand decreases from a five- to four-membered ring.[67] Venugopal has also prepared an acidic bismuth dication coordinated to a tridentate trispyrazolylborate ligand (**c**), which catalyzes the hydrosilylation of olefins under mild conditions.[68] Lichtenberg isolated a set of bismuth aminotroponiminate cations with varying substituents and counter-anions, and observed modest changes in acceptor numbers with anion exchange (**d**).[69] Recently, the Lewis acidity of a series of bismuth amides was evaluated using the Gutmann-Beckett method, with acceptor numbers as high as 69 (**e**).[70] These amides are capable of undergoing single- and double-CH activation reactions. Gabbai isolated a stibenium dication that catalyzes the hydrosilylation of benzaldehyde (**f**).[71] Very recently, Lichtenberg and coworkers synthesized cationic bismepines with substantially higher acceptor numbers than halobismepines (**g**).[66] The wide variability in reported acceptor numbers for antimony and bismuth complexes suggests that the Lewis acidity can be finely tuned to achieve desired reactivity.

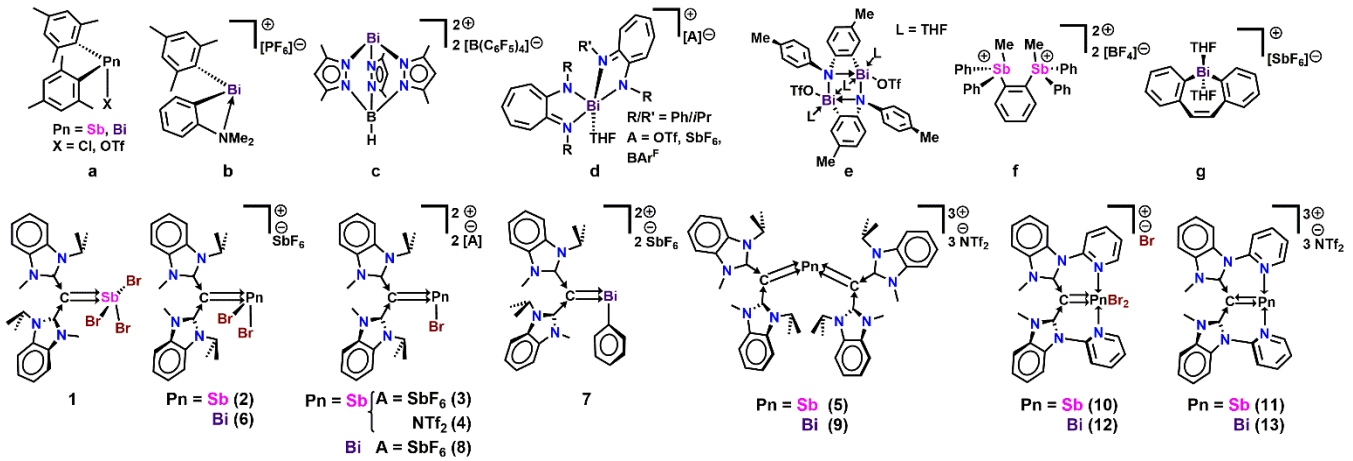

Compound	^{31}P NMR δ (ppm)	Acceptor Number	Solvent	Compound	^{31}P NMR δ (ppm)	Acceptor Number	Solvent
a	51-82	22-90	CD_2Cl_2	**4**	79	84	CD_2Cl_2
b	72	69	CD_2Cl_2	**5**	63	49	CD_2Cl_2
c	75	75	*o*-$Cl_2C_6D_4$	**6**	68	59	CD_2Cl_2
d	50-53	21-27	CD_2Cl_2	**7**	75	74	CD_2Cl_2
e	72	69	CH_2Cl_2	**8**	70	65	CD_2Cl_2
f	62	47	CH_2Cl_2	**9**	64	50	CD_2Cl_2
g	70	64	CH_2Cl_2	**10**	52	23	CD_3CN
1	54	28	CD_3CN	**11**	91	109	CD_3CN
2	60	42	CD_2Cl_2	**12**	51	23	CD_3CN
3	76	78	CD_3CN	**13**	79	84	CD_3CN

Figure 4. Cationic antimony and bismuth complexes that have been assessed using the Gutmann-Beckett method. ^{31}P NMR chemical shifts and corresponding acceptor numbers are given. For compounds **a**-**g**, ANs were compiled as reported or calculated using the formula AN = 2.21 x [$\delta(^{31}\text{P NMR})_{\text{sample}} - 41.0$].

Encouraged by these reports, comparative Lewis acidities of our pnictaalkene cations were probed using the Gutmann-Beckett method. One equivalent of triethylphosphine oxide ($O{=}PEt_3$) was added to a solution of each cation in CD_2Cl_2 or CD_3CN. In the interest of confirming the pnictogen atoms as the Lewis acidic sites in these cations, single crystals suitable for X-ray diffraction were isolated from reactions of triethylphosphine oxide and the bismuthenium ions **7** and **8**. One triethylphosphine oxide molecule coordinates to the phenyl-substituted Bi dication **7** (Figure 5). In this case, the Bi–O bond (2.253(3) Å) is shorter than the Bi–O bonds in **8** (2.312(5) and 2.319(4) Å). Interestingly, in the solid-state, two $O{=}PEt_3$ molecules coordinate to the **8** (Figure 5). As expected, an elongation in the Bi1–C1 bond is observed upon addition of $O{=}PEt_3$. Attempts to isolate single crystals of the $O{=}PEt_3$ adducts of the remaining cations were not successful.

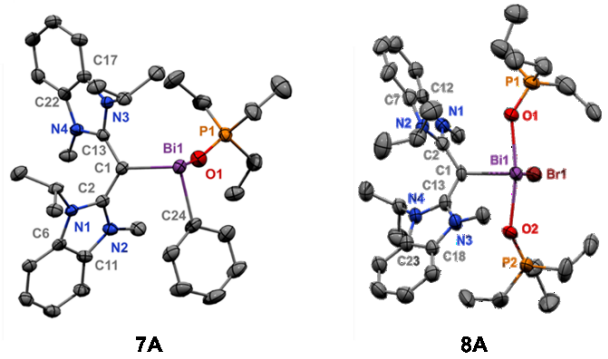

Figure 5. Molecular structures of compounds **7A** and **8A**. H atoms and counterions omitted for clarity. One DCM molecule that co-crystallized with **7A** is omitted for clarity. A monoprotonated CDC molecule co-crystallized with **8A** and is omitted for clarity, as are the minor positions of the disordered atoms. Thermal ellipsoids set at 50% probability. Selected

bond lengths (Å) and angles (°) for **7A**: Bi1–O1: 2.253(3); O1–P1: 1.517(4); Bi1–C1: 2.203(5); Bi1–C24: 2.226(5); O1–Bi1–C1: 91.74(15); O1–Bi1–C24: 88.76(16); **8A**: Bi1–O1: 2.312(5); O1–P1: 1.508(4); Bi1–O2: 2.319(4); O2–P2: 1.503(5); Bi1–Br1: 2.7085(8); Bi1–C1: 2.228(6); O1–Bi1–O2: 165.11(18); O1–Bi1–C1: 85.7(2).

The ^{31}P NMR chemical shifts and acceptor numbers for compounds **1**-**13** are reported in Figure 4. As expected, a significant increase in the AN is observed upon sequential bromide abstractions from compound **1** (AN = 28) to **2** (AN = 42) to **3** (AN = 78). Conversely, the trication **5** shows a marked decrease in the AN (AN = 49) as the second equivalent of CDC contributes significant electron density to Sb. The trend is the same for the analogous monodentate CDC Bi compounds, with the dication **7** having the highest AN (74). Interestingly, the AN for the Sb compound **3** (78) is much higher than **8** (65) – the bismuth analog of **4**. This reversal in expected Lewis acidity moving down the periodic table was recently observed in a set (mesityl)$_2$PnOTf (Pn = Sb or Bi) complexes reported by Venugopal.[46] Pellois and Gabbaï have also observed a reversal in Lewis acidity in a set of pnictogenium cations as evaluated using fluoride anion affinity.[45] Addition of one equivalent of O=PEt$_3$ to the stibenium trication **11** resulted in a sharp peak at 90.5 ppm in the ^{31}P NMR spectrum, which corresponds to an exceptionally high AN of 109. This AN is comparable to the quintessential Lewis acid BBr$_3$.[55] Compound **11** shows a significantly higher AN (109) than **10** (23), further demonstrating the increase in Lewis acidity upon halide abstraction. As predicted, **11** has a much higher AN than the trication **5** (49), which indicates that the pyridyl nitrogen groups in **11** contribute less to the electronic stability of Bi compared to a

second equivalent of CDC in **5**. Similarly, the tripositive bismuthenium ion **13** shows a much higher AN (84) compared to **12** (23). Compound **13** also shows a substantially higher AN than the trication **9** (50). As observed with compounds **4** and **8**, a reversal in the Lewis acidity is observed from bismuth (**13**) to antimony (**11**).

We also computed fluoride ion affinities (FIAs) for the tricationic complexes **11** and **13**, and compared with that of SbF_5 (see Figure S40 for the geometries of fluoride bound analogues). Since the FIA of a tricationic species in gas-phase would be large (311.6 (**11**) and 305.7 (**13**) kcal/mol) due to the strong ionic interaction and the stability from charge neutralization, we evaluated FIA in presence of DCM solvent using the polarizable continuum model (PCM), an implicit solvation model which is computationally cost-effective and provides reliable results. The FIA of SbF_5 in DCM solvent is 85.1 kcal/mol, whereas the FIA values for **11** and **13** are larger than SbF_5, being 99.8 and 94.3 kcal/mol, respectively. Therefore, they can be considered Lewis superacids.[72, 73] The energy decomposition analysis (EDA) for **11-F$^-$** and **13-F$^-$** complexes taking **11** or **13** as one fragment and F^- as another shows the factors which lead to the larger interaction energy in the former complex than the latter (see Table S3). Both the orbital (covalent) and electrostatic interactions are larger for Sb than Bi, although at the same time the larger Pauli repulsion for Sb makes the interaction energy only marginally larger in **11-F$^-$** than **13-F$^-$**.

We performed bonding analyses on compounds **1-5** and **10-13** with the minimum energy geometries at the BP86-D3(BJ)/def2-TZVP level of theory. The def2-TZVP basis set uses a quasi-relativistic pseudo-potential for 28 and 60 core electrons of Sb and Bi atom, respectively. The computed key geometrical parameters match well with the experimental values, and the deviation lies within the accuracy of the chosen level of theory and crystal

packing effect in the solid state (see Figure S41). The corresponding molecular orbitals (MOs) were examined with the same isosurface values responsible for Pn–C/N bonding (see Figure S42). It is well-established that CDC can readily employ its σ-lone pair for bonding.[34, 35, 38] However, CDC π-donation is generally weaker than σ-donation because its strength greatly depends on the shape, symmetry, and orientation of the accepting orbitals and the electrophilicity of the interacting unit. Therefore, they are often assigned as double dative interactions rather than bonds.[74] The present complexes, therefore, serve as perfect examples to study the effect of charge on the efficacy of Pn–C π-bonding. The corresponding MOs responsible for the Pn–C π-interaction (HOMO for **1-3** and **11-13**, HOMO-1 for **5** and **10**, Figure 6) show increasing participation of the Pn center in the π-bonding moving from the neutral compound (**1**) to the monocation (**2**) to the dication (**3**). Similarly, strong C–Sb–C π-bonding can be seen in the case of trication (**5**). This observation remains consistent for the (^{py}CDC)Pn cations; Pn–C π-bond strength increases moving from **10** to **11** and from **12** to **13**.

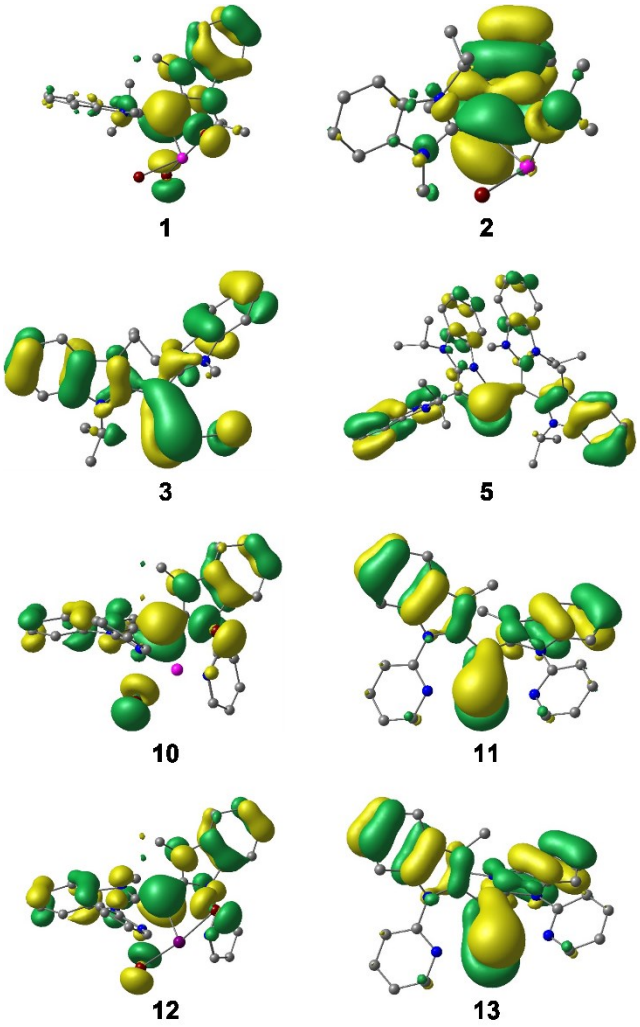

Figure 6. Corresponding molecular orbitals responsible for Pn–C π-bond formation in complexes **1**-**3** (HOMO), **5** (HOMO-1), **10** (HOMO-1), **11**-**13** (HOMO).

We then analyzed the topology of electron density in these complexes using quantum theory of atoms-in-molecules (QTAIM).[75] Figure 7 shows the contour plots of the Laplacian of electron density ($\nabla^2\rho(r)$) in **1-3** and **5** with a particular focus on the Sb–C bonds (see Figure S43 for others), where solid blue lines show the electron density depleted region and violet dotted lines represent the electron density accumulated region. The plots of $\nabla^2\rho(r)$ are quite similar in all cases with a large violet region around carbon, representing the lone-pair

of electrons that is polarized towards the electrophilic Sb centers. The bond critical points (BCP) for the Sb–C bonds lie just outside the electron accumulated region, and therefore, $\nabla^2\rho(r_c)$ is positive in all cases (a typical characteristic for bonds involving heavier elements). The total energy density ($H(r_c)$) is an effective descriptor for these cases.[76] $H(r_c)$ is negative for every compound, indicating covalent character in the Pn–C bonds. As the positive charge increases in the complex, the values of $H(r_c)$ become increasingly negative, signifying increased covalent character. Figure 7 also depicts the ellipticity values ($\varepsilon(r_c)$) at the Pn–C BCP, which gives important information about the double bond character of Pn–C bonds. Namely, single and triple bonds have cylindrical electron density distribution ($\varepsilon(r_c) \approx 0$), whereas for a double bond, because of asymmetric electron distribution, it has $\varepsilon(r_c)$ value greater than zero. In the case of **1**, the $\varepsilon(r_c)$ value at the BCP of Sb–C bond is 0.09. However, it is almost doubled in **2** (0.17) and is tripled in **3** (0.28), which corroborates with the MO and $H(r_c)$ data. The $\varepsilon(r_c)$ value is also high in **5** (0.23), but since it has two coordinated CDC ligands, the value cannot be compared to **3**. Similar increments in the $\varepsilon(r_c)$ value is noted moving from **10** to **11**, and from **12** to **13** (Figure S43). Note that because of Py to Pn π-donation, the $\varepsilon(r_c)$ value is also non-zero at the BCP of Pn–N bonds (Figure S43).

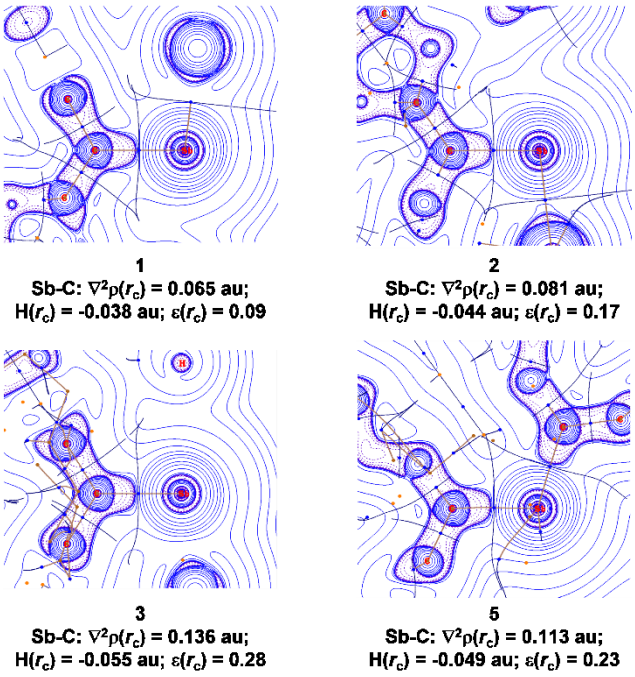

Figure 7. The contour plots of Laplacian of electron density ($\nabla^2(r)$) showing the C-Sb bond in compounds **1**-3 and **5** at the BP86-D3(BJ)/def2-TZVP level of theory. The blue solid lines show $\nabla^2(r) > 0$ region and violet dotted lines show $\nabla^2(r) < 0$ region.

To gain additional insight into the σ- and π-bond strengths, EDA in combination with natural orbital for chemical valence (NOCV) theory was employed. However, given the change in charge from the neutral to the tricationic complexes, the selection of the charge and electronic states of the interacting fragments is not trivial. Nonetheless, it has been shown that the size of the orbital interaction, ΔE_{orb}, can be used as an effective probe to dictate the best interacting scheme to represent a given bond. The fragments that give the smallest ΔE_{orb} value are the most appropriate ones for describing a bond because it indicates that the interacting fragments are the most closely aligned to those in the complex.[77, 78] Several possible bonding schemes were studied for the Sb and Bi cations (see Tables S4-S11).

For **1**, the neutral fragmentation leading to the donor-acceptor complex is the most reasonable one. For monocationic complexes **2**, **10** and **12**, CDC^{+} forms the electron-sharing σ-bond and dative π-bond with $SbBr_2$ or $BiBr_2$. In the dication (**3**) and trication (**5**), CDC^{2+} and $(CDC)_2^{2+}$ in the triplet state forms electron-sharing σ- and π-bonds with triplet SbBr and Sb^{+}, respectively. In the case of **3**, CDC^{2+} and SbBr in singlet states interacting through donor-acceptor interactions is another meaningful description of the bonding as revealed by the similar ΔE_{orb} value to CDC^{2+} and SbBr in triplet states. For the tricationic compounds **11** and **13**, the best description is that CDC^{2+} in the singlet state forms strong σ-dative bonds with singlet Sb^{+} and Bi^{+}, and p_π^2 electrons from Sb^{+} and Bi^{+} are also strongly backdonated to the empty π-orbital of CDC^{2+}. This scheme has slightly lower ΔE_{orb} values than the triplet-triplet scheme forming electron-sharing σ- and π-bonds. We further verified the choice of scheme at another level of theory, PBE0-D3(BJ)/TZ2P-ZORA//PBE0-D3(BJ)/def2-TZVP, to rule out any artifacts resulting from a particular level (Tables S12 and S13).

Tables S14-S21 show the numerical results of EDA-NOCV for the best scheme. The relative contributions of the ionic (ΔE_{elstat}) and covalent energy (ΔE_{orb}) terms show that for the neutral complex (**1**), the CDC–$SbBr_3$ bond is slightly more ionic in nature than covalent, but the reverse is true for the monocationic compounds. In fact, as the positive charge increases, the relative dominance of the covalent contribution over electrostatic also increases. For example, in the tricationic complexes, the covalent contribution is responsible for 72-76% of total attraction. The pair-wise orbital interactions, which give the strength of σ and π interactions, are given in Tables S14-S21. Figure 8 displays the deformation densities

corresponding to σ and π interactions along with their related ΔE_{orb} values. In this plot, electron density shifts from red to blue region. The general observation from Figure 8 is that CDC-Pn σ interaction is always very strong, regardless of the charge and bonding description, while the CDC-Pn π interaction is relatively weaker. In the case of **1**, the π bond strength is -10.3 kcal/mol. Moving from **1** to **2**, the strength slightly increases. However, the CDC–Pn π bond strength becomes much more significant in the dicationic and tricationic complexes. Therefore, the present results show a way to tune the π bond strength in CDC complexes by varying the cationic charge of the system.

1

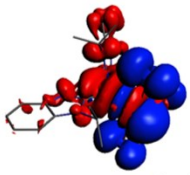

$\Delta E_{orb(1)}$ = -103.1; $|\nu_1|$ = 1.17

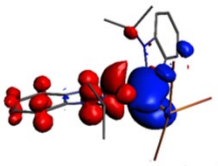

$\Delta E_{orb(2)}$ = -10.3; $|\nu_2|$ = 0.34

2

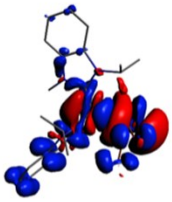

$\Delta E_{orb(1)}$ = -118.5; $|\nu_{1\alpha/1\beta}|$ = 0.72/0.52

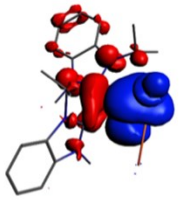

$\Delta E_{orb(2)}$ = -12.4; $|\nu_2|$ = 0.46

3

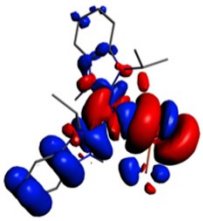

$\Delta E_{orb(1)}$ = -128.5; $|\nu_{1\alpha/1\beta}|$ = 0.76/0.49

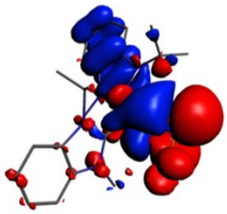

$\Delta E_{orb(2)}$ = -42.6; $|\nu_{2\alpha/2\beta}|$ = 0.77/0.56

5

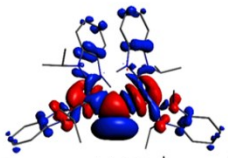

$\Delta E_{orb(1)}$ = -115.3; $|\nu_{1\alpha/1\beta}|$ = 0.68/0.58

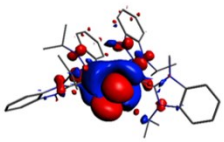

$\Delta E_{orb(2)}$ = -50.7; $|\nu_{2\alpha/2\beta}|$ = 0.68/0.62

10/(12)

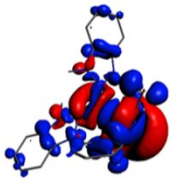

$\Delta E_{orb(1)}$ = -150.1(-130.9); $|\nu_{1\alpha/1\beta}|$ = 0.82/0.54(0.83/0.51))

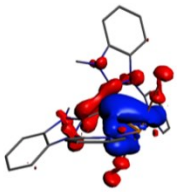

$\Delta E_{orb(2)}$ = -6.4(-5.2); $|\nu_2|$ = 0.24(0.22)

11/(13)

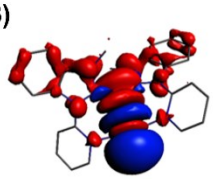

$\Delta E_{orb(1)}$ = -103.9(-87.6); $|\nu_1|$ = 1.03(0.99)

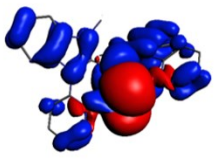

$\Delta E_{orb(2)}$ = -74.0(-76.9); $|\nu_2|$ = 1.54(1.56)

Figure 8. The plot of deformation densities corresponding to σ and π interactions of compounds **1**-**3**, **5**, and **10**-**13**. The corresponding ΔE_{orb} values are given in kcal/mol. The isosurface value is 0.0005 au. The size of the charge transfer is given by charge eigenvalue, ν.

CONCLUSIONS

Presented are the first examples of CDC-stibaalkene cations, which possess the shortest reported C=Sb^{+} bonds. Theoretical calculations support the presence of both σ and π interactions between the carbone carbon and Pn centers, of which the latter interaction is weaker than the former. Nonetheless, the dicationic and tricationic complexes exhibit very strong π-bonding. Formation of carbon-pnictogen double bonds in these complexes is achieved through non-reductive pathways enabled by strongly donating carbone ligands. The strong donor ability of carbones makes them excellent ligand platforms to prepare highly Lewis acidic complexes with p-block elements. This appears to be the first quantitative assessment of Lewis acidity among carbone-pnictenium ions, and the data obtained using the Gutmann-Beckett method indicate that these cations are comparable to or are stronger Lewis acids than known Sb and Bi cations. Indeed, the multidentate coordination of ^{py}CDC enables the preparation of highly Lewis acidic pnictenium trications with ANs up to 109, exceeding that of tricationic $[(CDC)_2Pn][NTf_2]_3$ compounds (ANs up to 50). These pnictenium trications can be considered Lewis superacids based on the calculated FIAs. Additionally, a reversal in the Lewis acidity from Bi to Sb is observed for the pnictenium trications **11** and **13** and pnictaalkene dications **4** and **8**. The trend of increasing Lewis acidity with sequential halide abstraction and the high ANs hint at a tunable platform

to explore chemical reactivity. Consequently, further study is warranted to investigate the potential of these cations in catalytic systems and as candidates to mediate bond activation. These studies are of interest to us and will be reported in due course.

EXPERIMENTAL SECTION

General Procedures

All manipulations were carried out under an atmosphere of purified argon using standard Schlenk techniques or in a MBRAUN LABmaster glovebox equipped with a –37 °C freezer. Deuterated solvents were purchased from Acros Organics and Cambridge Isotope Laboratories and dried the same way as their protic analogues. THF and hexanes were distilled over sodium/benzophenone. DCM and MeCN were distilled over CaH_2. Glassware was oven-dried at 190 °C overnight. NMR spectra were recorded at room temperature on a Varian Inova 500 MHz (^{1}H: 500.13 MHz, ^{31}P{^{1}H}: 202.46 MHz), a Varian NMRS 600 MHz (^{1}H: 600.13 MHz, ^{31}P{^{1}H}: 242.94 MHz) and a Bruker Avance 800 MHz spectrometer (^{1}H: 800.13 MHz, ^{13}C: 200.19 MHz). Proton and carbon chemical shifts are reported in ppm and are referenced using the residual proton and carbon signals of the deuterated solvent (^{1}H; CD_2Cl_2, δ 5.32, CD_3CN, δ 1.94, CD_3OD, δ 3.31, ^{13}C; CD_2Cl_2, δ 53.84, CD_3CN, 118.3). Phosphorus chemical shifts are reported in ppm and referenced using an external standard (85% H_3PO_4). Abbreviations are as follows; s = singlet, d = doublet, t = triplet, hept = heptet, dt = doublet of triplets, m = multiplet, br = broad. Elemental analyses were performed by Haleigh Machost at the University of Virginia Department of Chemistry using a Perkin Elmer 2400 Series II Instrument. The ligands CDC[47] and ^{py}CDC[50] were prepared following

reported procedures. Compounds **6**-**9** were prepared following modified literature procedures;[35] THF was excluded from these syntheses to prevent THF coordination to bismuth.

Synthesis of (CDC)$SbBr_3$ (1)

To a 20 mL scintillation vial, $SbBr_3$ (376 mg, 1.04 mmol) was added and stirred in 5 mL of THF. A solution of CDC (375 mg, 1.04 mmol) in 5 mL of THF was added dropwise to the stirring solution to afford the formation of a yellow precipitate. The solution was dried under reduced pressure to afford (CDC)$SbBr_3$ as a yellow solid (750 mg, yield >99%). Crystals suitable for X-ray diffraction were grown from a layered mixture of diethyl ether into a concentrated solution of **1** in DCM. NMR assignments correspond to the numeric positions labeled in Figure 9. ^{1}H NMR (600.13 MHz, CD_2Cl_2) δ: 7.60 (d, J = 7.9 Hz, 2H, H_4), 7.41 (m, 6H, $H_{1,2,3}$), 4.97 (hept, J = 7.0 Hz, 2H, N-C*H*-$(CH_3)_2$), 3.87 (s, 6H, N-C*H*$_3$), 1.53 (d, J = 7.0 Hz, 12H, N-CH-(C*H*$_3$)$_2$). ^{13}C NMR (201.19 MHz, CD_2Cl_2) δ: 156.9 ($C_{carbene}$), 133.9 (C_5), 130.3 (C_6), 125.1 ($C_{2,3}$), 114.0 (C_4), 111.6 (C_1), 52.3 (N-*C*H-$(CH_3)_2$), 34.6 (N-*C*H_3), 21.7 (N-CH-(*C*H_3)$_2$. Anal. calcd for $C_{23}H_{28}N_4SbBr_3$: C, 38.26, H, 3.91, N, 7.76%. Found: C, 37.95, H, 3.72, N, 7.49%.

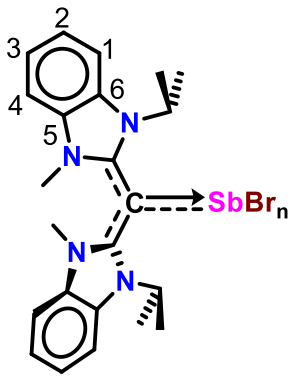

Figure 9. Aromatic proton and carbon NMR assignments are labeled using the numeric values above for **1**-**4**.

Synthesis of [(CDC)SbBr$_2$][SbF$_6$] (2)

To a 20 mL scintillation vial, (CDC)SbBr$_3$ (75 mg, 0.104 mmol) was added and stirred in 5 mL of DCM. In the dark, AgSbF$_6$ (35.7 mg, 0.104 mmol) was added to the stirring solution to afford an immediate color change from yellow to orange. After stirring for 2 hours, the solution was filtered and dried *in vacuo* to give [(CDC)SbBr$_2$][SbF$_6$] as an orange solid (71 mg, yield 77%). Orange crystals suitable for single crystal X-ray diffraction were obtained from a DCM/hexanes (1:1) mixture at room temperature. NMR assignments correspond to the numeric positions labeled in Figure 9. ^{1}H NMR (500.13 MHz, CD_2Cl_2) δ: 7.71 (d, J = 7.6 Hz, 2H, H_4), 7.54 (m, 6H, $H_{1,2,3}$), 4.79 (hept, J = 7.0 Hz, 2H, N-C*H*-$(CH_3)_2$), 3.83 (s, 6H, N-C*H*$_3$), 1.59 (d, J = 7.0 Hz, 12H, N-CH-(C*H*$_3$)$_2$). ^{13}C NMR (201.19 MHz, CD_2Cl_2) δ: 155.1 ($C_{carbene}$), 133.5 (C_5), 129.9 (C_6), 126.2 (br, $C_{2,3}$), 114.4 (C_4), 112.4 (C_1), 53.0 (N-*C*H-$(CH_3)_2$), 34.4 (N-*C*H$_3$), 21.6 (N-CH-(*C*H$_3$)$_2$. Anal. calcd for $C_{23}H_{28}N_4Sb_2Br_2F_6$: C, 31.47, H, 3.22, N, 6.38%. Found: C, 31.83, H, 3.26, N, 6.35%.

Synthesis of [(CDC)SbBr][SbF_6]$_2$ (3)

In a 20 mL scintillation vial, (CDC)$SbBr_3$ (75 mg, 0.104 mmol) was added and stirred in 5 mL of DCM. In the dark, $AgSbF_6$ (71.4 mg, 0.208 mmol) was added to the stirring solution to afford a color change from yellow to red. After stirring two hours, the solution was filtered. The filtrate was collected, and solvent was removed *in vacuo* to afford **3** as a red solid (95 mg, 89%). Crystals suitable for X-ray diffraction were grown from a layered mixture of hexanes/DCM. NMR assignments correspond to the numeric positions labeled in Figure 9. ^{1}H NMR (500.13 MHz, CD_3CN) δ: 7.82 (d, J = 8.2 Hz, 2H, H_4), 7.66 (d, J = 8.3 Hz, 2H, H_{aryl}), 7.54 (t, J = 7.5 Hz, 2H, H_{aryl}), 7.49 (t, J = 7.5 Hz, 2H, H_{aryl}), 4.60 (hept, J = 7.0Hz, 2H, N-C*H*-$(CH_3)_2$), 3.90 (s, 6H, N-C*H*$_3$), 1.48 (d, J = 7.0 Hz, 12H, N-CH-(C*H*$_3$)$_2$). ^{13}C NMR (201.19 MHz, CD_3CN) δ: 156.2 (C_{NHC}), 133.9 (C_5), 130.2 (C_6), 126.1 (C_2), 126.1 (C_3), 114.9 (C_4), 113.1 (C_1), 52.8 (N-*C*H-$(CH_3)_2$), 34.6 (N-*C*H$_3$), 20.9 (N-CH-(*C*H$_3$)$_2$). Anal. calcd for $C_{23}H_{28}N_4Sb_3BrF_{12}$: C, 26.73, H, 2.73, N, 5.42%. Found: C, 26.86, H, 2.87, N, 5.23%.

Synthesis of [(CDC)SbBr][NTf_2]$_2$ (4)

To a 20 mL scintillation vial, (CDC)$SbBr_3$ (100 mg, 0.139 mmol) was added and stirred in 5 mL of DCM. In the dark, $AgNTf_2$ (107.5 mg, 0.278 mmol) was added to the stirring solution to afford an immediate color change from yellow to red. After stirring for 2 hours, the solution was filtered and dried under reduced pressure to give [(CDC)SbBr][NTf_2]$_2$ as a red solid (136 mg, 87%). Red crystals suitable for single crystal X-ray diffraction were obtained from a DCM/hexanes (1:1) mixture at room temperature. NMR assignments correspond to the numeric positions labeled in Figure 9. ^{1}H NMR (500.13 MHz, CD_2Cl_2) δ: 7.80 (d, J = 9.0

Hz, 2H, H_4), 7.66-7.58 (m, 6H, $H_{1,2,3}$), 4.84 (br, 2H, N-C*H*-$(CH_3)_2$), 3.95 (s, 6H, N-C*H*$_3$), 1.58 (d, *J* = 6.4 Hz, 12H, N-CH-(C*H*$_3$)$_2$). ^{13}C NMR (201.19 MHz, CD_3CN) δ: 154.4 (C_{NHC}), 133.6 (C_5), 130.0 (C_6), 127.2 (C_2), 127.0 (C_3), 120.9 (quart, *J* = 320.6 Hz, C_{NTf2}), 115.4 (C_4), 113.9 (C_1), 52.9 (N-*C*H-$(CH_3)_2$), 34.4 (N-*C*H_3), 21.1 (N-CH-(*C*H_3)$_2$). Anal. calcd for $C_{27}H_{28}N_6SbF_{12}O_8S_4$: C, 28.89, H, 2.51, N, 7.49%. Found: C, 28.70, H, 2.63, N, 7.45%.

Synthesis of [(CDC)$_2$Sb][NTf$_2$]$_3$ (5)

To a 20 mL scintillation vial, (CDC)$SbBr_3$ (75 mg, 0.104 mmol) and CDC (37.5 mg, 0.104 mmol) were added and stirred in 5 mL of DCM. In the dark, $AgNTf_2$ (121.5 mg, 0.312 mmol) was added to the stirring solution to afford an immediate color change from yellow to purple. After stirring for 2 hours, the solution was filtered and dried under reduced pressure to give [(CDC)$_2$Sb][NTf$_2$]$_3$ as a purple solid (159 mg, yield 91%). Dark purple crystals suitable for single crystal X-ray diffraction were obtained from a DCM/hexanes (1:1) mixture at room temperature. NMR assignments correspond to the numeric positions labeled in Figure 10. ^{1}H NMR (600.13 MHz, CD_2Cl_2) δ: 7.97 (d, *J* = 7.8 Hz, 2H, $H_{4/10}$), 7.86 (d, *J* = 8.5 Hz, 2H, $H_{4/10}$), 7.73 (t, *J* = 7.8 Hz, 2H, $H_{2/3/8/9}$), 7.61 (m, 4H, $H_{2/3/8/9}$), 7.51 (d, *J* = 7.7 Hz, 2H, $H_{1/7}$), 7.48 (t, *J* = 8.1 Hz, 2H, $H_{2/3/8/9}$), 6.64 (d, *J* = 8.3 Hz, 2H, $H_{1/7}$), 5.92 (hept, *J* = 6.8 Hz, 2H, N-C*H*-$(CH_3)_2$), 4.56 (hept, *J* = 6.9 Hz, 2H, N-C*H*-$(CH_3)_2$), 3.32 (s, 6H, N-C*H*$_3$), 3.19 (s, 6H, N-C*H*$_3$), 2.09 (d, *J* = 7.0 Hz, 6H, N-CH-(C*H*$_3$)$_2$), 1.83 (d, *J* = 6.6 Hz, 6H, N-CH-(C*H*$_3$)$_2$), 1.78 (d, *J* = 6.8 Hz, 6H, N-CH-(C*H*$_3$)$_2$), 1.05 (d, *J* = 7.1 Hz, 6H, C-CH-(C*H*$_3$)$_2$). ^{13}C NMR (201.19 MHz, CD_2Cl_2) δ: 153.6 (C_{NHC}), 152.3 (C_{NHC}), 133.2 ($C_{5/6}$), 132.3 ($C_{5/6}$), 130.8 ($C_{11/12}$), 130.4 ($C_{11/12}$), 129.1 ($C_{2/3/8/9}$), 128.8 ($C_{2/3/8/9}$), 128.6 ($C_{2/3/8/9}$), 127.8 ($C_{2/3/8/9}$), 127.3 ($C_{2/3/8/9}$), 127.1 ($C_{2/3/8/9}$), 127.0 ($C_{2/3/8/9}$), 120.0 (quart,

J = 321.1 Hz, C_{NTf2}), 115.4 ($C_{4/10}$), 115.3 ($C_{4/10}$), 113.1 ($C_{1/7}$), 112.8 ($C_{1/7}$), 54.2 (N-*C*H-$(CH_3)_2$), 52.8 (N-*C*H-$(CH_3)_2$), 33.7 (N-*C*H_3), 32.6 (N-*C*H_3), 23.4 (N-CH-(*C*$H_3)_2$), 21.2 (N-CH-(*C*$H_3)_2$), 20.7 (N-CH-(*C*$H_3)_2$), 20.5 (N-CH-(*C*$H_3)_2$) Anal. calcd for $C_{52}H_{56}N_{11}SbF_{18}O_{12}S_6$: C, 37.11, H, 3.35, N, 9.15%. Found: C, 36.85, H, 3.51, N, 9.28%.

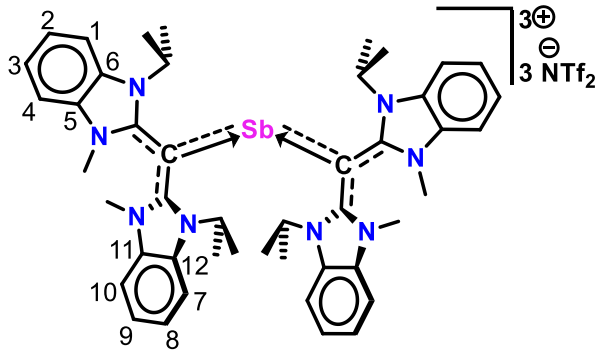

Figure 10. Aromatic proton and carbon NMR assignments are labeled using the numeric values above for **5**.

Synthesis of [(CDC^{py})SbBr$_2$][Br] (10)

To a 20 mL scintillation vial, $SbBr_3$ (88.1 mg, 0.244 mmol) and CDC^{py} (100 mg, 0.232 mmol) were added and stirred in 10 mL of THF to afford a yellow precipitate. After stirring for 2 hours, the supernatant was removed, and the solid was washed with Et_2O (2 x 5 mL). The solid was then dried under reduced pressure to give the product as a yellow solid. Yellow crystals suitable for single crystal X-ray diffraction were obtained from a DCM/hexanes layered mixture at room temperature. NMR assignments correspond to the numeric positions labeled in Figure 11. ^{1}H NMR (600.13 MHz, CD_3CN) δ: 9.01 (m, 2H, H_7), 8.46 (m, 2H, H_9), 8.26 (dt, J = 8.4 Hz, 2H, H_{10}), 7.88 (m, 2H, H_4), 7.83 (m, 2H, H_8), 7.62 (m, 2H, H_1), 7.59 (dt, J = 7.9 Hz, 2H, H_2), 7.55 (m, 2H, H_3), 3.25 (s, 6H, N-C*H*$_3$). ^{13}C NMR (201.19 MHz, CD_2Cl_2) δ:

153.2 (C_{NHC}), 148.8 (C_7), 146.6 (C_{11}), 145.7 (C_9), 133.7 (C_5), 130.7 (C_6), 127.6 (C_2), 126.5 (C_3), 125.6 (C_8), 121.2 (C_{10}), 114.1 (C_4), 112.9 (C_1), 33.8 (N-CH$_3$). Anal. calcd for $C_{27}H_{22}N_6SbBr_3$: C, 40.95, H, 2.80, N, 10.61%. Found: C, 40.45, H, 2.75, N, 10.51%.

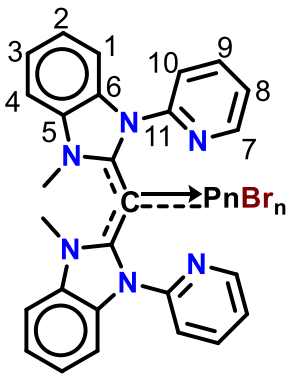

Figure 11. Aromatic proton and carbon NMR assignments are labeled using the numeric values above for **10**-**13**.

Synthesis of [(CDC^{py})Sb][NTf$_2$]$_3$ (11)

To a 20 mL scintillation vial, [(CDC^{py})SbBr$_2$][Br] (50.0 mg, 0.063 mmol) was added and stirred in 10 mL of 1,2-difluorobenzene. In the dark, AgNTf$_2$ (73.5 mg, 0.189 mmol) was added to the stirring solution to afford a subtle color change from yellow to yellow-orange. After stirring for 2 hours, the solution was filtered and dried under reduced pressure to give [CDC$_2$Sb][NTf$_2$]$_3$ as an orange solid (85 mg, yield 96%). Orange crystals suitable for single crystal X-ray diffraction were obtained from layering a 1,2-difluorobenzene/DCM (2:1) mixture with hexanes at room temperature. NMR assignments correspond to the numeric positions labeled in Figure 11. ^{1}H NMR (800.13 MHz, CD$_3$CN) δ: 8.98 (d, J = 4.6 Hz, 2H, H$_7$), 8.60 (t, J = 7.0 Hz, 2H, H$_9$), 8.40 (d, J = 8.1 Hz, 2H, H$_{10}$), 7.99 (t, J = 5.7 Hz, 2H, H$_8$), 7.94 (d, J

= 8.2 Hz, 2H, H_4), 7.72 (d, *J* = 8.1 Hz, 2H, H_1), 7.69 (t, *J* = 7.5 Hz, 2H, H_2), 7.63 (t, *J* = 7.0 Hz, 2H, H_3), 3.37 (s, 6H, N-C*H*$_3$). ^{13}C NMR (201.19 MHz, CD_3CN) δ: 151.1 (C_{NHC}), 148.5 (C_7), 146.9 (C_9), 145.9 (C_{11}), 133.7 (C_5), 130.5 (C_6), 128.4 (C_2), 127.3 (C_3), 126.8 (C_8), 122.4 (C_{10}), 120.9 (quart, *J* = 320.7 Hz, C_{NTf2}), 114.5 (C_4), 113.5 (C_1), 34.2 (N-*C*H$_3$). Anal. calcd for $C_{33}H_{22}F_{18}O_{12}N_9S_6Sb$: C, 28.46, H, 1.59, N, 9.05%. Found: C, 28.59, H, 1.56, N, 8.96%.

Synthesis of [(CDC^{py})BiBr$_2$][Br] (12)

To a 20 mL scintillation vial, $BiBr_3$ (75.0 mg, 0.167 mmol) and CDC^{py} (72.0 mg, 0.167 mmol) were added and stirred in 10 mL of THF to afford an orange precipitate. After stirring for 3 hours, the solution was dried under reduced pressure to give [(CDC^{py})BiBr$_2$][Br] as an orange solid (140 mg, yield 95%). Orange crystals suitable for single crystal X-ray diffraction were obtained from a DCM/hexanes (1:1) mixture at room temperature. NMR assignments correspond to the numeric positions labeled in Figure 11. ^{1}H NMR (600.13 MHz, CD_3OD) δ: 9.17 (dd, *J* = 5.4 Hz, 2H, H_7), 8.44 (m, 2H, H_9), 8.28 (d, *J* = 8.4 Hz, 2H, H_{10}), 7.84 (d, *J* = 8.4 Hz, 2H, H_4), 7.82 (m, 2H, H_8), 7.62-7.57 (m, 4H, $H_{1,2}$), 7.50 (m, 2H, H_3), 3.36 (s, 6H, N-C*H*$_3$). **Suitable ^{13}C NMR data could not be obtained due to poor solubility of **12** in even the most polar of solvents. Anal. calcd for $C_{27}H_{22}N_6BiBr_3$: C, 36.89, H, 2.52, N, 9.56%. Found: C, 36.91, H, 2.46, N, 9.21%.

Synthesis of [(CDC^{py})Bi][NTf$_2$]$_3$ (13)

To a 20 mL scintillation vial, [(CDC^{py})BiBr$_2$][Br] (35.0 mg, 0.040 mmol) was added and stirred in 10 mL of 1,2-difluorobenzene. In the dark, $AgNTf_2$ (46.4 mg, 0.120 mmol) was added to the stirring solution to afford a slight color change from orange to red. After stirring for 2

hours, the solution was filtered and dried under reduced pressure to give [(CDC^{py})Bi][NTf$_2$]$_3$ as a red-orange solid (57 mg, yield 97%). Red crystals suitable for single crystal X-ray diffraction were obtained from a 1,2-difluorobenzene/hexanes layered mixture at room temperature. NMR assignments correspond to the numeric positions labeled in Figure 11. ^{1}H NMR (500.13 MHz, CD$_3$CN) δ: 9.06 (d, *J* = 4.0 Hz, 2H, H$_7$), 8.47 (t, *J* = 7.6 Hz, 2H, H$_9$), 8.32 (d, *J* = 8.1 Hz, 2H, H$_{10}$), 7.89 (t, *J* = 6.5 Hz, 2H, H$_8$), 7.83 (d, *J* = 7.9 Hz, 2H, H$_4$), 7.66-7.61 (m, 4H, H$_{1,2}$), 7.53 (t, *J* = 6.9 Hz, 2H, H$_3$), 3.41 (s, 6H, N-C*H*$_3$). ^{13}C NMR (201.19 MHz, CD$_3$CN) δ: 153.5 (C$_{NHC}$), 150.2 (C$_7$), 146.8 (C$_{11}$), 145.6 (C$_9$), 133.7 (C$_5$), 131.0 (C$_6$), 127.9 (C$_2$), 126.8 (C$_3$), 122.3 (C$_{10}$), 120.8 (quart, *J* = 320.7 Hz, C$_{NTf2}$), 114.0 (C$_4$), 113.4 (C$_1$), 33.6 (N-*C*H$_3$). Anal. calcd for C$_{33}$H$_{22}$F$_{18}$O$_{12}$N$_9$S$_6$Bi: C, 26.78, H, 1.50, N, 8.52%. Found: C, 27.13, H, 1.49, N, 8.32%.

Reactions of carbodicarbene-pnictaalkene cations with triethylphosphine oxide:

In a J. Young NMR tube, O=PEt$_3$ was added to equimolar solutions of compounds **1**-**13** in CD$_2$Cl$_2$ or CD$_3$CN and shaken. ^{31}P NMR was subsequently taken of each solution to determine ^{31}P NMR chemical shifts.

Acceptor Number Calculation

Acceptor Numbers (ANs) were calculated using the following formula based on the ^{31}P NMR chemical shifts (δ_{sample}) for compounds **1**-**13**: AN = 2.21 ($\delta(^{31}P\ NMR)_{sample} - 41.0$)

ASSOCIATED CONTENT

Supporting Information.

The supporting information is available free of charge.

NMR spectra of compounds **1**-**5** and **10**-**13**, Gutmann-Beckett ^{31}P NMR spectra of compounds **1**-**13**, crystallographic and X-ray refinement details, and computational details (PDF).

Accession Codes

CCDC 2156966-2156976 contain the supplementary crystallographic data for this paper. These data can be obtained free of charge from The Cambridge Crystallographic Data Centre via www.ccdc.cam.ac.uk/structures, or by emailing data_request@ccdc.cam.ac.uk, or by contacting The Cambridge Crystallographic Data Centre, 12 Union Road, Cambridge CB2 1EZ, UK; fax: +44 1223 336033.

AUTHOR INFORMATION

Corresponding Authors

Robert J. Gilliard, Jr. – Department of Chemistry, University of Virginia, McCormick Road, PO Box 400319, Charlottesville, Virginia 22904, USA; E-mail: rjg8s@virginia.edu

Sudip Pan – Philipps-Universität Marburg Hans-Meerwein-Straße, 35032 Marburg, Germany; E-mail: pans@chemie.uni-marburg.de

Author Contributions

L.S.W. led the experimental work, including conducting the synthesis, characterization, and Gutmann-Beckett (GB) experiments of compounds **1**-**5** and **10**-**13**. J.E.W. prepared compounds **6**-**9** and conducted Gutmann-Beckett (GB) experiments for those complexes.

D.A.D. helped refine and solve the crystal structures and provided crystallographic details in the supporting information. W.T. performed the electron density analysis. S.P. performed energy decomposition analysis, analysed the computational results and wrote the theoretical discussion. R.J.G. conceived and directed the project. All authors contributed to the preparation of the manuscript.

Notes

The authors declare no competing financial interest.

ACKNOWLEDGMENT

We are grateful to the University of Virginia (UVA) and the American Chemical Society Petroleum Research Fund (62280-DNI3) for support of this work. W.T. thanks the financial support of the National Agency for Research and Development (ANID) through FONDECYT projects 1211128.

REFERENCES

1. Lipshultz, J. M.; Li, G.; Radosevich, A. T., Main Group Redox Catalysis of Organopnictogens: Vertical Periodic Trends and Emerging Opportunities in Group 15. *J. Am. Chem. Soc.* **2021,** *143* (4), 1699-1721.

2. Moon, H. W.; Cornella, J., Bismuth Redox Catalysis: An Emerging Main-Group Platform for Organic Synthesis. *ACS Catalysis* **2022,** *12* (2), 1382-1393.

3. Abbenseth, J.; Goicoechea, J. M., Recent developments in the chemistry of non-trigonal pnictogen pincer compounds: from bonding to catalysis. *Chem. Sci.* **2020,** *11* (36), 9728-9740.

4. Kumar, V.; Gonnade, R. G.; Yildiz, C. B.; Majumdar, M., Stabilization of the Elusive Antimony(I) Cation and Its Coordination Complexes with Transition Metals. *Angew. Chem.* **2021,** *133* (48), 25726-25733.

5. Marczenko, K. M.; Chitnis, S. S., Bismuthanylstibanes. *Chem. Commun.* **2020,** *56* (58), 8015-8018.

6. Kindervater, M. B.; Hynes, T.; Marczenko, K. M.; Chitnis, S. S., Squeezing Bi: PNP and P2N3 pincer complexes of bismuth. *Dalton Trans.* **2020,** *49* (45), 16072-16076.

7. Pyykkö, P., Additive Covalent Radii for Single-, Double-, and Triple-Bonded Molecules and Tetrahedrally Bonded Crystals: A Summary. *J. Phys. Chem. A* **2015,** *119* (11), 2326-2337.

8. Bondi, A., van der Waals Volumes and Radii. *J. Phys. Chem.* **1964,** *68* (3), 441-451.

9. Wang, Z. L.; Hu, H. S.; Szentpály, L.; Stoll, H.; Fritzsche, S.; Pyykkö, P.; Schwarz, W. H. E.; Li, J., Understanding the Uniqueness of 2p Elements in Periodic Tables. *Chem. Eur. J.* **2020,** *26* (67), 15558-15564.

10. Desclaux, J. P., Relativistic Dirac-Fock expectation values for atoms with Z = 1 to Z = 120. *At. Data Nucl. Data Tables* **1973,** *12* (4), 311-406.

11. Jurrat, M.; Maggi, L.; Lewis, W.; Ball, L. T., Modular bismacycles for the selective C–H arylation of phenols and naphthols. *Nature Chemistry* **2020,** *12* (3), 260-269.

12. Planas, O.; Wang, F.; Leutzsch, M.; Cornella, J., Fluorination of arylboronic esters enabled by bismuth redox catalysis. *Science* **2020,** *367* (6475), 313-317.

13. Pang, Y.; Leutzsch, M.; Nöthling, N.; Cornella, J., Catalytic Activation of N2O at a Low-Valent Bismuth Redox Platform. *J. Am. Chem. Soc.* **2020,** *142* (46), 19473-19479.

14. Planas, O.; Peciukenas, V.; Cornella, J., Bismuth-Catalyzed Oxidative Coupling of Arylboronic Acids with Triflate and Nonaflate Salts. *J. Am. Chem. Soc.* **2020,** *142* (26), 11382-11387.

15. Nesterov, V.; Reiter, D.; Bag, P.; Frisch, P.; Holzner, R.; Porzelt, A.; Inoue, S., NHCs in Main Group Chemistry. *Chem. Rev.* **2018,** *118* (19), 9678-9842.

16. Deka, R.; Orthaber, A., Carbene chemistry of arsenic, antimony, and bismuth: origin, evolution and future prospects. *Dalton Trans.* **2022**.

17. Philipp, M. S. M.; Krahfuss, M. J.; Radacki, K.; Radius, U., N-Heterocyclic Carbene and Cyclic (Alkyl)(amino)carbene Adducts of Antimony(III). *Eur. J. Inorg. Chem.* **2021,** *2021* (38), 4007-4019.

18. Waters, J. B.; Chen, Q.; Everitt, T. A.; Goicoechea, J. M., N-Heterocyclic carbene adducts of the heavier group 15 tribromides. Normal to abnormal isomerism and bromide ion abstraction. *Dalton Trans.* **2017,** *46* (36), 12053-12066.

19. Kretschmer, R.; Ruiz, D. A.; Moore, C. E.; Rheingold, A. L.; Bertrand, G., One-, Two-, and Three-Electron Reduction of a Cyclic Alkyl(amino)carbene–SbCl3 Adduct. *Angew. Chem. Int. Ed.* **2014,** *53* (31), 8176-8179.

20. Arduengo III, A. J.; Krafczyk, R.; Schmutzler, R.; Mahler, W.; Marshall, W. J., A Tris(trifluoromethyl)antimony Adduct of a Nucleophilic Carbene: Geometric Distortions in Carbene Adducts. *Z. Anorg. Allg. Chem.* **1999,** *625* (11), 1813-1817.

21. Aprile, A.; Corbo, R.; Vin Tan, K.; Wilson, D. J. D.; Dutton, J. L., The first bismuth–NHC complexes. *Dalton Trans.* **2014,** *43* (2), 764-768.

22. Siddiqui, M. M.; Sarkar, S. K.; Nazish, M.; Morganti, M.; Köhler, C.; Cai, J.; Zhao, L.; Herbst-Irmer, R.; Stalke, D.; Frenking, G.; Roesky, H. W., Donor-Stabilized Antimony(I) and Bismuth(I) Ions: Heavier Valence Isoelectronic Analogues of Carbones. *J. Am. Chem. Soc.* **2021,** *143* (3), 1301-1306.

23. Wang, G.; Freeman, L. A.; Dickie, D. A.; Mokrai, R.; Benkő, Z.; Gilliard, R. J., Highly Reactive Cyclic(alkyl)(amino) Carbene- and *N* -Heterocyclic Carbene-Bismuth(III) Complexes: Synthesis, Structure, and Computations. *Inorg. Chem.* **2018,** *57* (18), 11687-11695.

24. Wang, G.; Freeman, L. A.; Dickie, D. A.; Mokrai, R.; Benkő, Z.; Gilliard Jr., R. J., Isolation of Cyclic(Alkyl)(Amino) Carbene–Bismuthinidene Mediated by a Beryllium(0) Complex. *Chem. Eur. J.* **2019,** *25* (17), 4335-4339.

25. Zhang, J.; Wei, J.; Ding, W.-Y.; Li, S.; Xiang, S.-H.; Tan, B., Asymmetric Pnictogen-Bonding Catalysis: Transfer Hydrogenation by a Chiral Antimony(V) Cation/Anion Pair. *J. Am. Chem. Soc.* **2021,** *143* (17), 6382-6387.

26. Yang, M.; Hirai, M.; Gabbaï, F. P., Phosphonium–stibonium and bis-stibonium cations as pnictogen-bonding catalysts for the transfer hydrogenation of quinolines. *Dalton Trans.* **2019,** *48* (20), 6685-6689.

27. Ugarte, R. A.; Devarajan, D.; M. Mushinski, R.; W. Hudnall, T., Antimony(v) cations for the selective catalytic transformation of aldehydes into symmetric ethers, α,β-unsaturated aldehydes, and 1,3,5-trioxanes. *Dalton Trans.* **2016,** *45* (27), 11150-11161.

28. Ramler, J.; Poater, J.; Hirsch, F.; Ritschel, B.; Fischer, I.; Bickelhaupt, F. M.; Lichtenberg, C., Carbon monoxide insertion at a heavy p-block element: unprecedented formation of a cationic bismuth carbamoyl. *Chem. Sci.* **2019,** *10* (15), 4169-4176.

29. Qiu, R.; Yin, S.; Zhang, X.; Xia, J.; Xu, X.; Luo, S., Synthesis and structure of an air-stable cationic organobismuth complex and its use as a highly efficient catalyst for the direct diastereoselective Mannich reaction in water. *Chem. Commun.* **2009,** (31), 4759-4761.

30. Chitnis, S. S.; Robertson, A. P. M.; Burford, N.; Patrick, B. O.; McDonald, R.; Ferguson, M. J., Bipyridine complexes of E3+(E = P, As, Sb, Bi): strong Lewis acids, sources of E(OTf)3and synthons for EI and EV cations. *Chem. Sci.* **2015,** *6* (11), 6545-6555.

31. Dyker, C. A.; Lavallo, V.; Donnadieu, B.; Bertrand, G., Synthesis of an Extremely Bent Acyclic Allene (A "Carbodicarbene"): A Strong Donor Ligand. *Angew. Chem. Int. Ed.* **2008,** *47* (17), 3206-3209.

32. Ramirez, F.; Desai, N. B.; Hansen, B.; McKelvie, N., Hexaphenylcarbodiphosphorane, (C6H5)3PCP(C6H5)3. *J. Am. Chem. Soc.* **1961,** *83* (16), 3539-3540.

33. Münzer, J. E.; Kneusels, N.-J. H.; Weinert, B.; Neumüller, B.; Kuzu, I., Hexaphenyl carbodiphosphorane adducts of heavier group 15 element trichlorides: syntheses, properties and reactivities. *Dalton Trans.* **2019,** *48* (29), 11076-11085.

34. Hollister, K. K.; Molino, A.; Breiner, G.; Walley, J. E.; Wentz, K. E.; Conley, A. M.; Dickie, D. A.; Wilson, D. J. D.; Gilliard, R. J., Air-Stable Thermoluminescent Carbodicarbene-Borafluorenium Ions. *J. Am. Chem. Soc.* **2022,** *144* (1), 590-598.

35. Walley, J.; Warring, L.; Wang, G.; Dickie, D. A.; Pan, S.; Frenking, G.; Gilliard, R. J., Carbodicarbene Bismaalkene Cations: Unravelling the Complexities of Carbene versus Carbone in Heavy Pnictogen Chemistry. *Angew. Chem. Int. Ed.* **2021,** *60*, 6682-6690.

36. Chen, W.-C.; Lee, C.-Y.; Lin, B.-C.; Hsu, Y.-C.; Shen, J.-S.; Hsu, C.-P.; Yap, G. P. A.; Ong, T.-G., The Elusive Three-Coordinate Dicationic Hydrido Boron Complex. *J. Am. Chem. Soc.* **2014,** *136* (3), 914-917.

37. Chen, W.-C.; Shih, W.-C.; Jurca, T.; Zhao, L.; Andrada, D. M.; Peng, C.-J.; Chang, C.-C.; Liu, S.-K.; Wang, Y.-P.; Wen, Y.-S.; Yap, G. P. A.; Hsu, C.-P.; Frenking, G.; Ong, T.-G., Carbodicarbenes: Unexpected π-Accepting Ability during Reactivity with Small Molecules. *J. Am. Chem. Soc.* **2017,** *139* (36), 12830-12836.

38. Walley, J. E.; Breiner, G.; Wang, G.; Dickie, D. A.; Molino, A.; Dutton, J. L.; Wilson, D. J. D.; Gilliard, J. R. J., s-Block carbodicarbene chemistry: C(sp3)–H activation and cyclization mediated by a beryllium center. *Chem. Commun.* **2019,** *55* (13), 1967-1970.

39. Đorđević, N.; Ganguly, R.; Petković, M.; Vidović, D., Bis(carbodicarbene)phosphenium trication: the case against hypervalency. *Chem. Commun.* **2016,** *52* (63), 9789-9792.

40. Đorđević, N.; Ganguly, R.; Petković, M.; Vidović, D., E–H (E = B, Si, C) Bond Activation by Tuning Structural and Electronic Properties of Phosphenium Cations. *Inorg. Chem.* **2017,** *56* (23), 14671-14681.

41. Petz, W.; Dehnicke, K.; Holzmann, N.; Frenking, G.; Neumüller, B., The Reaction of BeCl2 with Carbodiphosphorane C(PPh3)2; Experimental and Theoretical Studies. *Z. Anorg. Allg. Chem.* **2011,** *637* (12), 1702-1710.

42. Petz, W.; Öxler, F.; Neumüller, B.; Tonner, R.; Frenking, G., Carbodiphosphorane C(PPh 3) 2 as a Single and Twofold Lewis Base with Boranes: Synthesis, Crystal Structures and Theoretical Studies on [H3B{C(PPh3). *Eur. J. Inorg. Chem.* **2009,** *2009* (29-30), 4507-4517.

43. Inés, B.; Patil, M.; Carreras, J.; Goddard, R.; Thiel, W.; Alcarazo, M., Synthesis, Structure, and Reactivity of a Dihydrido Borenium Cation. *Angew. Chem. Int. Ed.* **2011,** *50* (36), 8400-8403.

44. Sindlinger, C. P.; Stasch, A.; Wesemann, L., Heavy Group 15 Element Compounds of a Sterically Demanding Bis(iminophosphorane)methanide and -methanediide. *Organometallics* **2014,** *33* (1), 322-328.

45. Park, G.; Brock, D. J.; Pellois, J.-P.; Gabbaï, F. P., Heavy Pnictogenium Cations as Transmembrane Anion Transporters in Vesicles and Erythrocytes. *Chem* **2019,** *5* (8), 2215-2227.

46. Sharma, D.; Balasubramaniam, S.; Kumar, S.; Jemmis, E. D.; Venugopal, A., Reversing Lewis acidity from bismuth to antimony. *Chem. Commun.* **2021,** *57*, 8889-8892.

47. Chen, W.-C.; Hsu, Y.-C.; Lee, C.-Y.; Yap, G. P. A.; Ong, T.-G., Synthetic Modification of Acyclic Bent Allenes (Carbodicarbenes) and Further Studies on Their Structural Implications and Reactivities. *Organometallics* **2013,** *32* (8), 2435-2442.

48. NMR data was collected in CD3CN for compound 3 versus CD2Cl2 for compounds 1, 2, and 4.

49. Engesser, T. A.; Lichtenthaler, M. R.; Schleep, M.; Krossing, I., Reactive p-block cations stabilized by weakly coordinating anions. *Chem. Soc. Rev.* **2016,** *45* (4), 789-899.

50. Hsu, Y.-C.; Shen, J.-S.; Lin, B.-C.; Chen, W.-C.; Chan, Y.-T.; Ching, W.-M.; Yap, G. P. A.; Hsu, C.-P.; Ong, T.-G., Synthesis and Isolation of an Acyclic Tridentate Bis(pyridine)carbodicarbene and Studies on Its Structural Implications and Reactivities. *Angew. Chem.* **2015,** *127* (8), 2450-2454.

51. Bothwell, J. M.; Krabbe, S. W.; Mohan, R. S., Applications of bismuth(iii) compounds in organic synthesis. *Chem. Soc. Rev.* **2011,** *40* (9), 4649.

52. Erdmann, P.; Leitner, J.; Schwarz, J.; Greb, L., An Extensive Set of Accurate Fluoride Ion Affinities for p-Block Element Lewis Acids and Basic Design Principles for Strong Fluoride Ion Acceptors. *ChemPhysChem* **2020,** *21* (10), 987-994.

53. Marczenko, K. M.; Jee, S.; Chitnis, S. S., High Lewis Acidity at Planar, Trivalent, and Neutral Bismuth Centers. *Organometallics* **2020,** *39* (23), 4287-4296.

54. Erdmann, P.; Greb, L., Multidimensional Lewis Acidity: A Consistent Data Set of Chloride, Hydride, Methide, Water and Ammonia Affinities for 183 p-Block Element Lewis Acids. *ChemPhysChem* **2021,** *22* (10), 935-943.

55. Sivaev, I. B.; Bregadze, V. I., Lewis acidity of boron compounds. *Coord. Chem. Rev.* **2014,** *270-271*, 75-88.

56. Zhou, J.; Kim, H.; Liu, L. L.; Cao, L. L.; Stephan, D. W., An arene-stabilized η5-pentamethylcyclopentadienyl antimony dication acts as a source of Sb+ or Sb3+ cations. *Chem. Commun.* **2020,** *56* (85), 12953-12956.

57. Zhou, J.; Liu, L. L.; Cao, L. L.; Stephan, D. W., Nitrogen-Based Lewis Acids: Synthesis and Reactivity of a Cyclic (Alkyl)(Amino)Nitrenium Cation. *Angew. Chem. Int. Ed.* **2018,** *57* (13), 3322-3326.

58. Beckett, M. A.; Strickland, G. C.; Holland, J. R.; Sukumar Varma, K., A convenient n.m.r. method for the measurement of Lewis acidity at boron centres: correlation of reaction rates of Lewis acid initiated epoxide polymerizations with Lewis acidity. *Polymer* **1996,** *37* (20), 4629-4631.

59. Mayer, U.; Gutmann, V.; Gerger, W., The acceptor number — A quantitative empirical parameter for the electrophilic properties of solvents. *Monatsh. Chem.* **1975,** *106* (6), 1235-1257.

60. Ramler, J.; Lichtenberg, C., Molecular Bismuth Cations: Assessment of Soft Lewis Acidity. *Chem. Eur. J.* **2020,** *26* (45), 10250-10258.

61. Ramler, J.; Stoy, A.; Preitschopf, T.; Kettner, J.; Fischer, I.; Roling, B.; Fantuzzi, F.; Lichtenberg, C., Dihalo bismuth cations: unusual coordination properties and inverse solvent effects in Lewis acidity. *Chem. Commun.* **2022,** *58* (70), 9826-9829.

62. Erdmann, P.; Greb, L., What Distinguishes the Strength and the Effect of a Lewis Acid: Analysis of the Gutmann–Beckett Method. *Angew. Chem.* **2021**.

63. Lichtenberg, C., Molecular bismuth(III) monocations: structure, bonding, reactivity, and catalysis. *Chem. Commun.* **2021,** *57* (37), 4483-4495.

64. Répichet, S.; Le Roux, C.; Roques, N.; Dubac, J., BiCl3-catalyzed Friedel–Crafts acylation reactions: bismuth(III) oxychloride as a water insensitive and recyclable procatalyst. *Tetrahedron Lett.* **2003,** *44* (10), 2037-2040.

65. Wei, H.; Qian, G.; Xia, Y.; Li, K.; Li, Y.; Li, W., BiCl3-Catalyzed Hydroamination of Norbornene with Aromatic Amines. *Eur. J. Org. Chem.* **2007,** *2007* (27), 4471-4474.

66. Ramler, J.; Hofmann, K.; Lichtenberg, C., Neutral and Cationic Bismuth Compounds: Structure, Heteroaromaticity, and Lewis Acidity of Bismepines. *Inorg. Chem.* **2020,** *59* (6), 3367-3376.

67. Kannan, R.; Kumar, S.; Andrews, A. P.; Jemmis, E. D.; Venugopal, A., Consequence of Ligand Bite Angle on Bismuth Lewis Acidity. *Inorg. Chem.* **2017,** *56* (16), 9391-9395.

68. Balasubramaniam, S.; Kumar, S.; Andrews, A. P.; Varghese, B.; Jemmis, E. D.; Venugopal, A., A Dicationic Bismuth(III) Lewis Acid: Catalytic Hydrosilylation of Olefins. *Eur. J. Inorg. Chem.* **2019,** (28), 3265-3269.

69. Hanft, A.; Radacki, K.; Lichtenberg, C., Cationic Bismuth Aminotroponiminates: Charge Controls Redox Properties. *Chem. Eur. J.* **2021,** *27* (20), 6230-6239.

70. Oberdorf, K.; Grenzer, P.; Wieprecht, N.; Ramler, J.; Hanft, A.; Rempel, A.; Stoy, A.; Radacki, K.; Lichtenberg, C., CH Activation of Cationic Bismuth Amides: Heteroaromaticity, Derivatization, and Lewis Acidity. *Inorg. Chem.* **2021,** *60* (24), 19086-19097.

71. Hirai, M.; Cho, J.; Gabbaï, F. P., Promoting the Hydrosilylation of Benzaldehyde by Using a Dicationic Antimony-Based Lewis Acid: Evidence for the Double Electrophilic Activation of the Carbonyl Substrate. *Chem. Eur. J.* **2016,** *22* (19), 6537-6541.

72. Greb, L., Lewis Superacids: Classifications, Candidates, and Applications. *Chem. Eur. J.* **2018,** *24* (68), 17881-17896.

73. Müller, L. O.; Himmel, D.; Stauffer, J.; Steinfeld, G.; Slattery, J.; Santiso-Quiñones, G.; Brecht, V.; Krossing, I., Simple Access to the Non-Oxidizing Lewis Superacid PhF→Al(ORF)3 (RF=C(CF3)3). *Angew. Chem. Int. Ed.* **2008,** *47* (40), 7659-7663.

74. Su, W.; Pan, S.; Sun, X.; Zhao, L.; Frenking, G.; Zhu, C., Cerium–carbon dative interactions supported by carbodiphosphorane. *Dalton Trans.* **2019,** *48* (42), 16108-16114.

75. Bader, R. F. W., *Atoms in Molecules: A Quantum Theory*. Clarendon Press: Oxford, UK, 1990.

76. Cremer, D.; Kraka, E., Chemical Bonds without Bonding Electron Density ? Does the Difference Electron-Density Analysis Suffice for a Description of the Chemical Bond? *Angew. Chem., Int. Ed. Engl.* **1984,** *23* (8), 627-628.

77. Bickelhaupt, F. M.; Fonseca Guerra, C.; Mitoraj, M.; Sagan, F.; Michalak, A.; Pan, S.; Frenking, G., Clarifying notes on the bonding analysis adopted by the energy decomposition analysis. *Physical Chemistry Chemical Physics* **2022,** *24* (26), 15726-15735.

78. Pan, S.; Frenking, G., Comment on "Realization of Lewis Basic Sodium Anion in the NaBH 3 – Cluster". *Angew. Chem.* **2020,** *132* (23), 8836-8839.

For Table of Contents Only

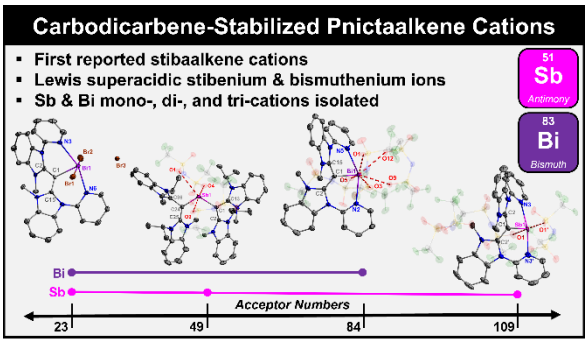

SYNOPSIS

The first examples of carbodicarbene-stibaalkene cations have been synthesized. The Lewis acidity of these cations and their bismuth analogs was evaluated using the Gutmann-Beckett

method. The unique bonding situations in these antimony and bismuth cations have been thoroughly assessed using experimental and computational methods. Two of the tricationic complexes presented are Lewis superacids as determined by fluoride ion affinity.